ADVANCES IN ATMOSPHERIC SCIENCES, VOL. 32, APRIL 2015, 553–564

Diurnal and Seasonal Variations of CO_2 Fluxes and Their Climate Controlling Factors for a Subtropical Forest in Ningxiang

JIA Binghao[1], XIE Zhenghui[*1], ZENG Yujin[1,2], WANG Linying[1,2], WANG Yuanyuan[1,2], XIE Jinbo[1,2], and XIE Zhipeng[1,2]

[1]*State Key Laboratory of Numerical Modeling for Atmospheric Sciences and Geophysical Fluid Dynamics, Institute of Atmospheric Physics, Chinese Academy of Sciences, Beijing* 100029

[2]*University of Chinese Academy of Sciences, Beijing* 100049

(Received 3 April 2014; revised 22 July 2014, accepted 28 July 2014)

ABSTRACT

In this study, the diurnal and seasonal variations of CO_2 fluxes in a subtropical mixed evergreen forest in Ningxiang of Hunan Province, part of the East Asian monsoon region, were quantified for the first time. The fluxes were based on eddy covariance measurements from a newly initiated flux tower. The relationship between the CO_2 fluxes and climate factors was also analyzed. The results showed that the target ecosystem appeared to be a clear carbon sink in 2013, with integrated net ecosystem CO_2 exchange (NEE), ecosystem respiration (RE), and gross ecosystem productivity (GEP) of −428.8, 1534.8 and 1963.6 g C m^{-2} yr^{-1}, respectively. The net carbon uptake (i.e. the −NEE), RE and GEP showed obvious seasonal variability, and were lower in winter and under drought conditions and higher in the growing season. The minimum NEE occurred on 12 June (−7.4 g C m^{-2} d^{-1}), due mainly to strong radiation, adequate moisture, and moderate temperature; while a very low net CO_2 uptake occurred in August (9 g C m^{-2} $month^{-1}$), attributable to extreme summer drought. In addition, the NEE and GEP showed obvious diurnal variability that changed with the seasons. In winter, solar radiation and temperature were the main controlling factors for GEP, while the soil water content and vapor pressure deficit were the controlling factors in summer. Furthermore, the daytime NEE was mainly limited by the water-stress effect under dry and warm atmospheric conditions, rather than by the direct temperature-stress effect.

Key words: net ecosystem exchange, diurnal and seasonal variations, climate controlling factors, subtropical mixed forest, East Asian monsoon region

Citation: Jia, B. H., Z. H. Xie, Y. J. Zeng, L. Y. Wang, Y. Y. Wang, J. B. Xie, and Z. P. Xie, 2015: Diurnal and seasonal variations of CO_2 fluxes and their climate controlling factors for a subtropical forest in Ningxiang. *Adv. Atmos. Sci.*, **32**(4), 553–564, doi: 10.1007/s00376-014-4069-4.

1. Introduction

Accurate estimation of land–atmosphere CO_2 flux is essential to understanding the feedback between the terrestrial biosphere and the atmosphere, in the context of global climate change and climate policy-making (Ju et al., 2007; Luo et al., 2009; Yuan et al., 2009; Piao et al., 2009; Xu et al., 2012; Le Quéré et al., 2013). The eddy covariance (EC) technique is one of the best methods for directly measuring the CO_2 flux of forest, grassland, and cropland ecosystems (Falge et al., 2001; Yu et al., 2006). A number of international networks have been established to monitor the carbon cycle in the terrestrial environment using this method. As a major network measuring the net ecosystem CO_2 exchange (NEE), FLUXNET (www.fluxdata.org) plays an important role in exploring soil–plant–atmosphere interactions, evaluating the role of terrestrial ecosystems in the global carbon cycle, and investigating the response of terrestrial ecosystem carbon exchange to global climate change (Baldocchi et al., 2001). At present, FLUXNET contains over 500 tower sites operated on a long-term and continuous basis, encompassing all the major biomes of the world. As an important part of FLUXNET, ChinaFLUX has taken the lead in flux observation and research in China, and has developed close communication and cooperation with other regional flux networks since its establishment (Yu et al., 2006). Moreover, it has offered new opportunities to quantify the temporal dynamics and environmental drivers of the carbon budget in the typical ecosystems of the East Asian monsoon region. However, the observation network is still too sparse for terrestrial carbon cycle studies of regions, continents, or the globe. Recently, many new flux measurement sites have been set up by other scientific institutes and universities in China, which are expected to enhance greatly the extent and intensity of CO_2 flux research over East Asia (Yu et al., 2006; Zheng et al., 2008;

* Corresponding author: XIE Zhenghui
Email: zxie@lasg.iap.ac.cn

Gao et al., 2009).

In August 2012, a field experimental observatory was established in Ningxiang (eastern Hunan Province, southern China), where a set of micrometeorological and eddy covariance instruments were installed. This site is surrounded by a mixed evergreen forest over a hilly zone and is located in the subtropical East Asian monsoon region. The CO_2 flux data from this site is intended to aid understanding of the carbon budget in the East Asian subtropical forest ecosystem and improve the terrestrial carbon cycle model. Liu et al. (2013) have already briefly introduced the site and presented a preliminary analysis of field observations collected from August to November 2012. Continuous measurements for more than one year have been collected so far, and are expected to provide data to quantify the temporal dynamics of CO_2 fluxes over subtropical forest. However, Falge et al. (2001) showed that the average data coverage from EC measurements during a year is usually less than 65% due to system failures or data rejection. These fragmented datasets may contain sufficient information for half-hourly model fitting, but completeness is needed for daily and annual sums, which are of widespread interest, e.g., to estimate ecosystem carbon budgets, to evaluate process model predictions, and for comparison with biometric measurements (Moffat et al., 2007; Du et al., 2014). Therefore, gap-filling procedures are required to provide complete datasets (Falge et al., 2001).

In this study, our primary objective is to establish quality control and gap-filling procedures to provide complete datasets from the Ningxiang site for terrestrial carbon cycle research. Furthermore, we examine diurnal and seasonal variations in the NEE and its component fluxes, gross ecosystem productivity (GEP) and total ecosystem respiration (RE). Finally, the relationship between the CO_2 fluxes and climate factors will be explored. This study should enhance our understanding of carbon exchange features and soil–plant–atmosphere interactions, especially the effect of dry and warm atmospheric conditions on NEE, for evergreen forest in the East Asian monsoon region. Moreover, these analyses provide observational evidence for the improvement of the terrestrial carbon cycle model.

2. Materials and methods

2.1. *Site description*

In August 2012, a field experimental observatory was established over a hilly zone in Ningxiang County (28°20′N, 112°34′E; 110 m above sea level). This site is about 36 km from Changsha city, eastern Hunan Province, southern China, in the East Asian monsoon region (Liu et al., 2013). Its terrain is relatively flat with homogeneous underlying surface and similar vegetation. The forest is a semi-natural ecosystem, over 40 years old. The total area of the forest is about 1 km^2 and the average vegetation height is about 7 m. The main vegetation types surrounding this site are mixed evergreen broadleaf and needleleaf forests, and the main species are *Pinus massoniana*, *Cunninghamia lanceolata*, and *Cinnamomum camphora*. The climate of the area is subtropical, and the climate data from the Changsha Weather Station, run by the China Meteorological Administration, close to this site, indicate that the annual mean precipitation is 1458 mm and the air temperature is 17.6°C (Liu et al., 2013).

2.2. *Data observation and post-processing*

A 20 m flux tower was set up at the Ningxiang site, selected based on favorable conditions for EC measurements in terms of regular terrain and homogeneity of land surface cover. Instruments for EC measurements, including a three-dimensional sonic anemometer (CSAT3, Campbell Scientific, Logan, UT, USA) and an open-path infrared CO_2 and H_2O analyzer (EC150, Campbell Scientific, Logan, UT, USA), were installed 17.5 m above the ground. At the same height, solar radiation components were measured by 4-Component Net Radiation Sensor (CNR4, Kipp & Zonen, Delft, NL). The CO_2 flux and radiation data were recorded by a CR3000 data logger (Campbell Scientific, Logan, UT, USA) with a 10 Hz sampling frequency, and averaged over 30 minute intervals. In addition, the tower was equipped with a series of meteorological instruments for measuring precipitation at the top of the tower, and air temperature, and relative humidity at 13.5 m above the ground. Soil water content and temperature were measured at various depths (0.05, 0.1, 0.2, 0.4, 0.6, 0.8 and 1.0 m). More detailed information about these instruments can be found in Liu et al. (2013). All these meteorological data were recorded by a CR1000 (Campbell Scientific, Logan, UT, USA) data logger and every 10 minutes. It should be noted that meteorological and flux measurements from 1 January to 31 December 2013 were used for data processing and analysis in this study.

The EC measurements were affected by both random errors, caused by sensor noise and instantaneous changes in atmospheric turbulence, and systematic biases, caused by sensor drift, limited instrument response, and selective systematic deviations caused by advection or storage (Aubinet et al., 2000; Baldocchi et al., 2001; Chen et al., 2013). Therefore, it was necessary to apply post-processing and quality control to the CO_2 flux measurements. Figure 1 shows a flowchart of the quality-control and gap-filling processing for the 30 minute CO_2 flux data. First, to eliminate the influence of horizontal and vertical advection in the mass-conservation equation, the raw 30 minute CO_2 flux data were converted by a three-dimensional coordinate rotation that aligned the vertical velocity measurement normal to the mean wind streamline and brought the mean lateral and vertical velocities to zero (Wilczak et al., 2001; Liu et al., 2006). Second, the effect of density fluctuations caused by correlated heat and water vapor fluctuations on the NEE was corrected [the WPL correction (Webb et al., 1980)], and abnormal data related to precipitation or dew and negative nighttime CO_2 flux data (photosynthesis does not occur in the dark) were eliminated.

To avoid the systemic underestimation of storage and advection due to relatively stable air stratification during the nighttime, which may lead to unrealistic NEE measurements using the EC sensors, the average value test method (AVT)

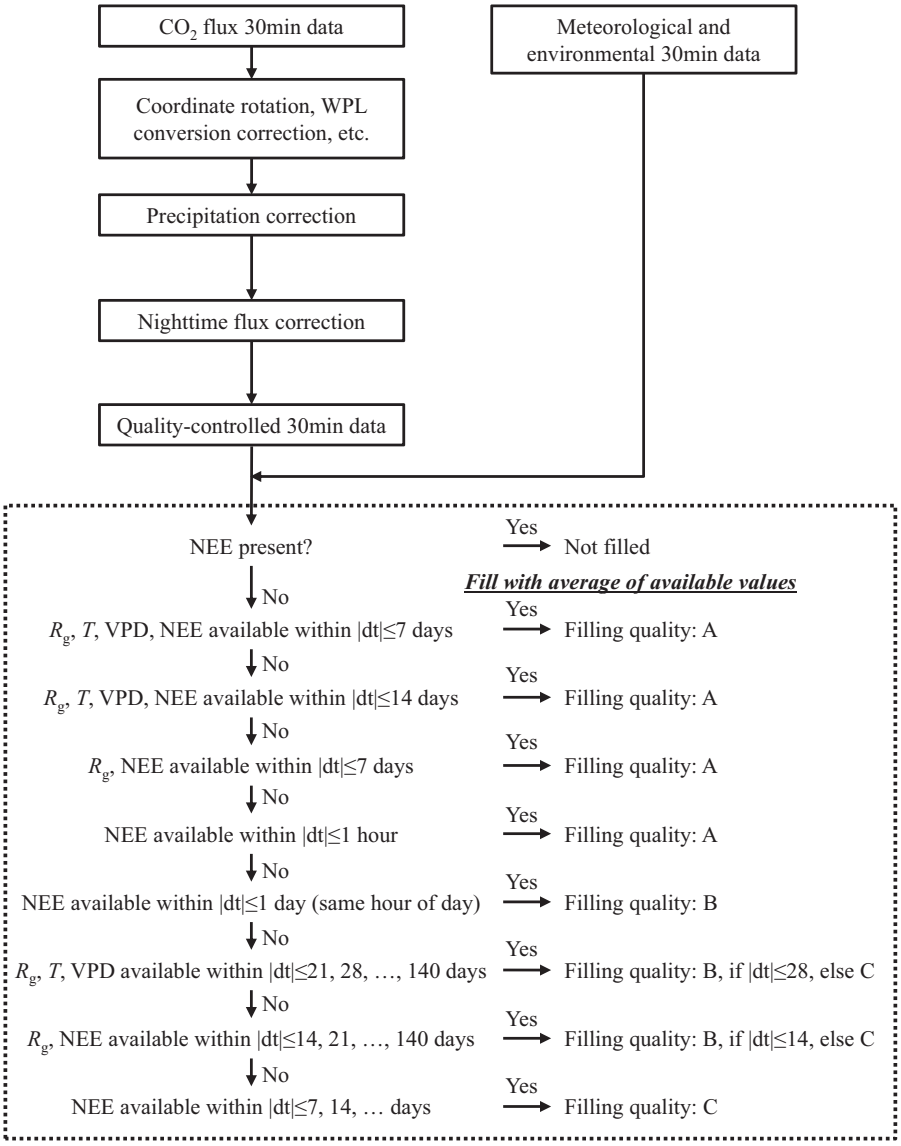

Fig. 1. Flow diagram of the quality-control and gap-filling algorithms used in this study. Abbreviations: NEE, net ecosystem CO_2 exchange; R_g, global radiation; T, air temperature; VPD, vapor pressure deficit; and $|dt|$, absolute difference in time. Filling qualities: A, high; B, medium; and C, low.

(Zhu et al., 2006) was used in this study to generate the friction velocity threshold (u_c) below which the data were rejected. The relationship between the average of nighttime NEE and friction velocity (u) is presented in Fig. 2. F_{c1} (solid line with dots) represents the change in the piecewise averaged nighttime CO_2 flux within different u ranges (0.01 m s^{-1} interval) for the four seasons (winter, spring, summer, autumn), and F_{c2} (solid line with triangles) is the accumulative recalculated average of these F_{c1}, using the values larger than u at this point. It is clearly found from Fig. 2 that nighttime NEE increases quickly with increasing u when u is low, especially in autumn (Fig. 2d). This demonstrates that the effect of lack of turbulence on the underestimation of nighttime NEE could not be ignored. According to the AVT method, a statistical variable T was calculated using the equation (Zhu et al., 2006):

$$T = \frac{|F_{c1} - F_{c2}|}{\sigma/\sqrt{n}}\,, \tag{1}$$

where σ is the standard deviation, and n the number of samples of F_{c1}. According to the principle of u_c determination and referring to Eq. (1) and Fig. 2, it was appropriate to set u_c to 0.17 m s^{-1} for winter, 0.2 m s^{-1} for spring, 0.21 m s^{-1} for summer, and 0.22 m s^{-1} for autumn. To obtain credible nighttime EC measurements, data for which the friction velocity was less than u_c were deleted to avoid underestimation (Zhu et al., 2006; Papale et al., 2006). In addition, the frequency distribution of u and the percentage of effective nighttime CO_2 flux data to all nighttime data at different u_c are also shown in Fig. 2 (right column, 0.05 m s^{-1} interval).

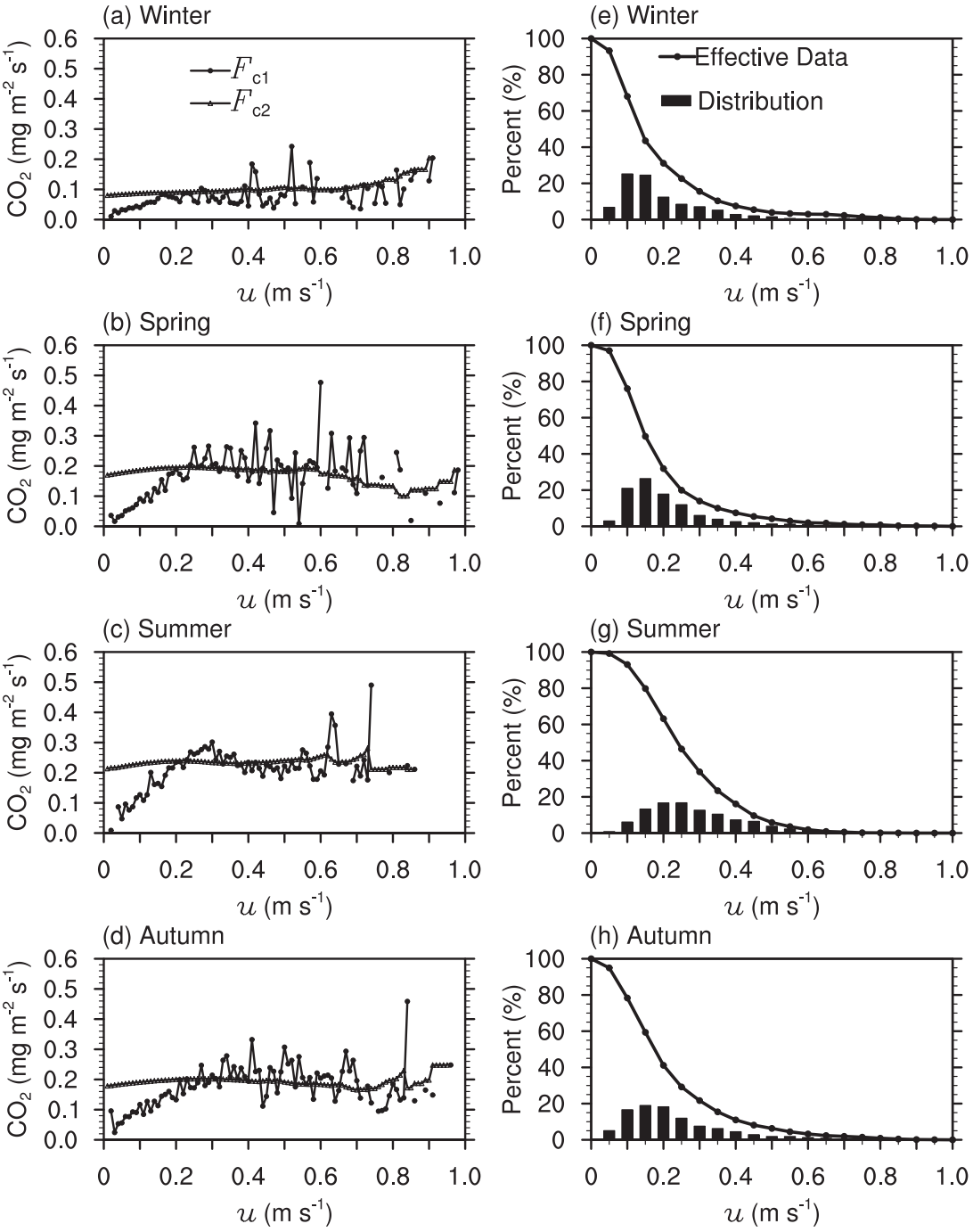

Fig. 2. (a–d) Relationship between the average nighttime CO_2 flux and friction velocity (u), and (e–h) the frequency distribution of u (bars) and the ratio of effective data (line) for the four seasons (winter, spring, summer, and autumn) in 2013. F_{c1} (solid line with dots) represents the change in the piecewise averaged nighttime CO_2 flux within different u ranges (0.01 m s^{-1} interval), and F_{c2} (solid line with triangles) is the accumulative recalculated average of these F_{c1}, using the values larger than u at this point; the distribution of u and the ratio of effective data to all nighttime data at different u_c was determined with a 0.05 m s^{-1} interval.

It is clearly found that the ratio of the effective NEE data decreased with the increase of u_c. For example, when u_c was set to the values mentioned above, about 60% of nighttime NEE data had to be corrected or filled, except during summer (40%). This indicates that the choice of u_c plays an important role in NEE estimations (Zhu et al., 2006).

2.3. *Gap filling*

After quality control, the average NEE data coverage for 2013 decreased to only 61% from 85%. Therefore, gap-filling procedures were used to provide complete datasets. Various gap-filling techniques are available and have been previously compared using measured data from multiple sites

(Moffat et al., 2007; Du et al., 2014). As an improved type of standard look-up table (Falge et al., 2001), the marginal distribution sampling (MDS) method (Reichstein et al., 2005) has shown a consistently high gap-filling performance and low annual sum bias (Moffat et al., 2007; Du et al., 2014). Moreover, it was adopted as one of the standard gap-filling techniques by the CarboEurope project and FLUXNET (Papale et al., 2006). Therefore, the MDS technique was used in this study to reproduce CO_2 flux data for the Ningxiang site.

The dotted box in Fig. 1 shows a flowchart of the MDS algorithm, in which gap filling for CO_2 flux and meteorological data was performed using methods similar to those of Falge et al. (2001), but also considered the co-variation of fluxes with meteorological variables and the temporal autocorrelation of the fluxes (Reichstein et al., 2005). A more detailed description of this algorithm can be found in Appendix A of Reichstein et al. (2005).

2.4. *Separation of NEE into assimilation and respiration*

The measured NEE from EC reflects the balance between GEP and RE (including autotrophic and heterotrophic respiration) and can be expressed as:

$$\mathrm{NEE} = \mathrm{RE} - \mathrm{GEP}\,. \tag{2}$$

To understand the mechanistic responses of ecosystem processes to environmental change, it was necessary to acquire estimates of the two main components RE and GEP of NEE through a so-called flux-partitioning algorithm.

The algorithm introduced by Reichstein et al. (2005) was used in this study to separate NEE into the two components RE and GEP. All the available RE data were estimated from air or soil temperature using the exponential regression model from Lloyd and Taylor (1994),

$$\mathrm{RE}(t) = \mathrm{RE}_{\mathrm{ref}}(t) e^{E_0[1/(T_{\mathrm{ref}}-T_0)-1/(T(t)-T_0)]}\,, \tag{3}$$

where $\mathrm{RE}_{\mathrm{ref}}$ is the base respiration at the reference temperature (T_{ref}, 10°C); E_0 is a temperature sensitivity parameter (189.01 K in this study); T_0 is kept constant at −46.02°C; and T is air or soil temperature. Air temperature was chosen in this study, the same as that made in Reichstein et al. (2005). Compared to that in Lloyd and Taylor (1994), the algorithm from Reichstein et al. (2005) defined a short-term temperature sensitivity (E_0) of RE, which could largely avoid the bias introduced by confounding factors in seasonal data. Moreover, the $\mathrm{RE}_{\mathrm{ref}}$ parameter was assumed to be temporally varying.

3. Results

3.1. *Seasonal dynamics of environmental factors*

Because the study site, Ningxiang, is located in the East Asian subtropical monsoon climate zone, the climate conditions show obvious seasonal dynamics (Fig. 3). Precipitation occurs mainly in April, May and June, and higher temperatures occur in summer (Fig. 3a). According to 26-year average statistics (1987–2012) from a meteorological station (28°13′N, 112°55′E) in Changsha, approximately 36 km southeast of the Ningxiang site, precipitation is concentrated mainly in spring and early summer, and the highest temperatures occur in July and August. Compared to the climatic average annual precipitation (1458 mm), the total precipitation for 2013 was lower (1056 mm), especially for July and August, which had only 4 and 27 mm precipitation respectively, much less than the average (157 and 110 mm). Moreover, air temperatures during these two months in 2013 were 2°C higher than average values, although the annual mean (18.2°C) was close to the climatic value (17.6°C). This suggests that a severe summer drought and high temperature stress occurred in 2013.

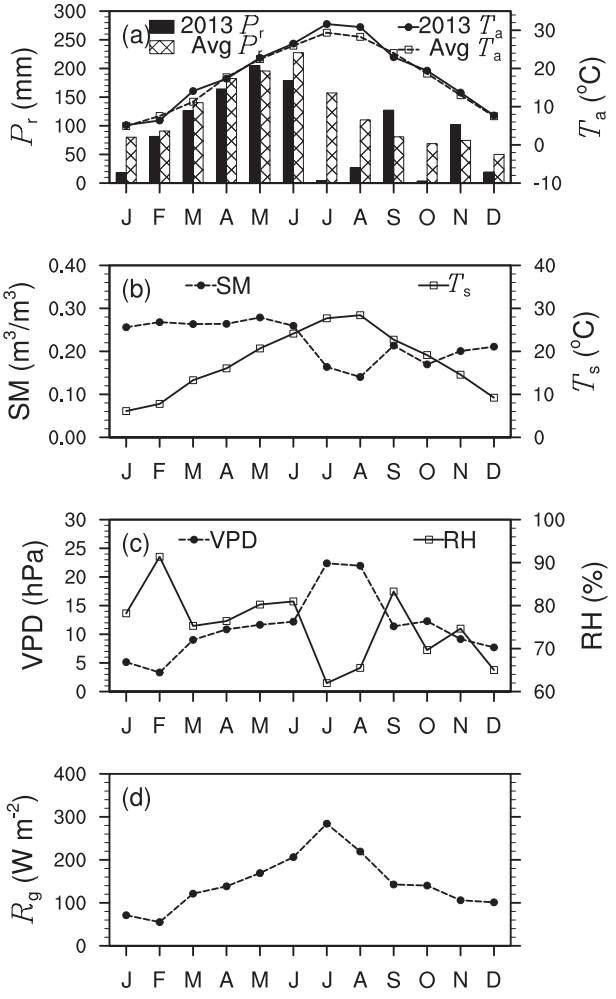

Fig. 3. Seasonal dynamics of (a) precipitation (P_r, bar plot) and air temperature (T_a, solid line) and the 26 year average (Avg, 1987–2012) from the nearest meteorological station (36 km away), (b) soil moisture (SM, dashed line) and temperature (T_s, solid line), (c) vapor pressure deficit (VPD, dashed line) and relative humidity (RH, solid line), and (d) global radiation (R_g).

In addition, it can be clearly observed from Fig. 3b that the soil water content (5 cm, dashed line) varied in a similar way to precipitation, showing an obvious decrease in July

and August due to the drought. Soil temperature (5 cm, solid line) had similar seasonal dynamics to air temperature (Figs. 3a and b). The maximum values of vapor pressure deficit (VPD), the difference (deficit) between the amount of moisture in the air and how much moisture the air can hold when it is saturated, occurred in July and August. It was largely attributed to the effect of the drought (lower relative humidity Fig. 3c) and high temperatures. The incoming global radiation (R_g) was highly seasonal, with minima in the cold season and maxima during the warm season (Fig. 3d).

3.2. *Diurnal and seasonal variations of CO_2 fluxes*

One of the main advantages of the EC measurement is its contribution to seasonal variation of CO_2 fluxes. Daily ecosystem CO_2 fluxes from the target site in 2013 accessed by the EC method are presented in Fig. 4, in which the 30 minute RE and GEP were obtained from flux partitioning of NEE data using the method shown in Fig. 1 at first, after which the daily mean values were then calculated. As shown in Fig. 4a, the respiration rate at the reference conditions (RE_{ref}) was expected to vary seasonally to avoid the bias introduced by confounding factors in seasonal data, such as plant phenological patterns, soil moisture (Joo et al., 2012), decomposition and/or soil microbial growth dynamics (Reichstein et al., 2005). This parameter was estimated for consecutive 4-day periods by the nonlinear regression model [Eq. (3)] after the determination of the parameter E_0, fixing all parameters except RE_{ref}. It should be noted that the regression analyses were performed using ordinary least squares regression that maximizes the likelihood of the parameter values under the assumption of normally distributed residuals (Reichstein et al., 2005). When the RE_{ref} was estimated for each period, they were then linearly interpolated between the estimates, which resulted in a dense time series of RE_{ref} (Reichstein et al., 2005). The strong increase in June 2013 and subsequent decrease of RE_{ref} may be related to fast growth-processes during this period (Reichstein et al., 2005).

It can be observed from Fig. 4b that NEE, RE and GEP showed obvious seasonal variability; NEE was higher in winter and under drought conditions and lower in the growing season, while RE and GEP showed the opposite seasonal variability. Furthermore, the seasonal variation in NEE was driven by both seasonal variations of GEP and RE. In addition, NEE was negative during most of the target periods, suggesting strong carbon fixation in the ecosystem. The maximum rate of net CO_2 uptake was 7.4 g C m^{-2} d^{-1} (12 June), due mainly to appropriate climate conditions for photosynthesis, including strong radiation (338 W m^{-2}), moderate air temperature (23.4°C), and adequate moisture (VPD and soil water content of 14 hPa and 0.27 m^3 m^{-3} respectively), which induced the highest GEP (14.4 g C m^{-2} d^{-1}) of the whole year. During the summer drought period (July and August), lower precipitation (Fig. 3a) led to low soil water content and atmospheric moisture. The drought seemed more severe in August, showing the lowest soil water content (less than 0.14 m^3 m^{-3}, Fig. 3b) during the whole year. Meanwhile, high temperature stress induced an increase

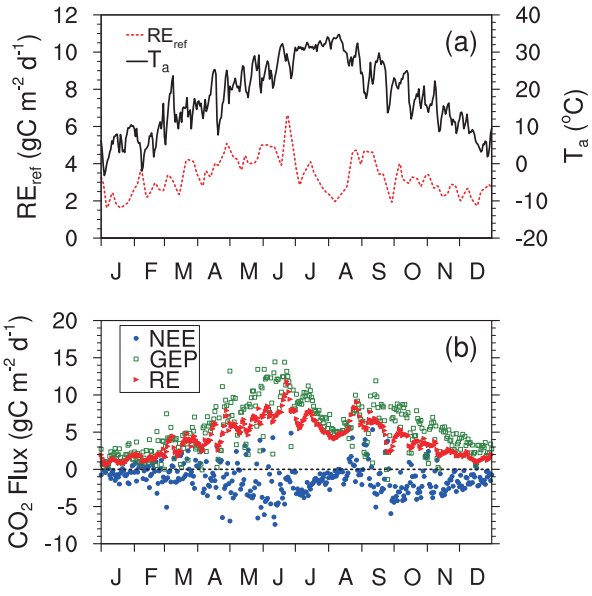

Fig. 4. Seasonal variations of (a) RE_{ref} (red dashed line), air temperature (T_a, black solid line), and (b) NEE (blue dots), GEP (green squares), RE (red triangles) for 2013. RE_{ref} is the base respiration at the reference temperature [10°C, Eq. (3)]; negative values for NEE indicate that the ecosystem is acting as a carbon sink.

in RE and strengthened the increase in VPD. Higher VPD increases transpirational demand and limits photosynthesis through stomatal closure (Farquhar and Sharkey, 1982). All these environmental conditions led to a very low net CO_2 uptake (absolute value) in August (9 g C m^{-2} $month^{-1}$), even less than in January (15 g C m^{-2} $month^{-1}$). However, the magnitude of carbon uptake (GEP) was still larger than carbon release (RE) during July–August. During the early growing season (April–June), adequate precipitation and radiation (Fig. 3) led to large carbon uptake because of the fast growth of these subtropical forests; although weak photosynthesis in the cold seasons, the ecosystem respiration was also low due to the limit of low temperature. Therefore, the target forest ecosystem functioned as an obvious carbon sink in 2013, even though it was affected by the summer drought. In general, on a yearly basis, the NEE, RE, and GEP were −428.8, 1534.8 and 1963.6 g C m^{-2} yr^{-1} respectively.

Figure 5 compares the diurnal variations of CO_2 fluxes during different months. There were evident diurnal variation patterns of daytime uptake and nighttime release for NEE. NEE moved from a positive value (release) to a negative value (uptake) after dawn, and then the CO_2 assimilation rate achieved the highest value between 1100 and 1200 local standard time (LST); and afterwards it began to decrease. This change was related to variations in total solar radiation and photosynthetically active radiation, caused by variations in the solar zenith angle throughout the day (Zhao et al., 2006). In addition, an obvious seasonality of monthly diurnal variation in NEE and GEP could be observed from Fig. 5, with a lower amplitude in winter and the drought season and higher amplitude in the growing season. When the

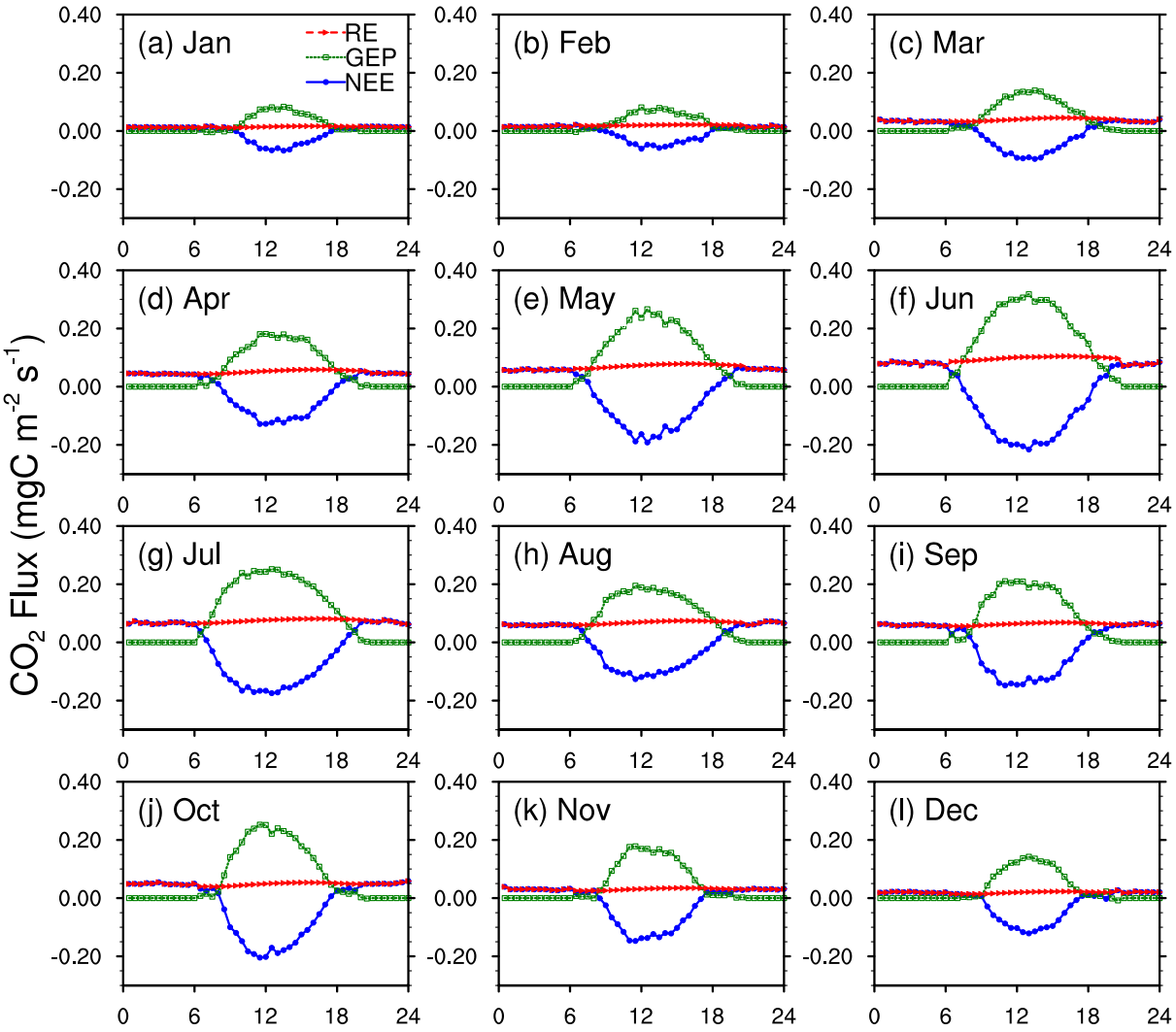

Fig. 5. Monthly diurnal variation of NEE (blue dots), GEP (green squares), and RE (red triangles).

solar zenith angle was high during the growing season, the duration of negative values in NEE was long. On the contrary, it was short in the cold seasons (Zhao et al., 2006). It was also found that the GEP showed a similar diurnal variation to NEE, of which the diurnal range was about 0.05–0.3 mg C m^{-2} s^{-1}, while RE showed smaller diurnal variations (0.005–0.05 mg C m^{-2} s^{-1}, Fig. 5). The main reasons for the low diurnal range of RE were perhaps the biases between estimated nighttime RE and observed NEE, and the weak diurnal variation in air temperature (3°C –7°C).

4. Environmental controls on CO_2 fluxes

4.1. *Effect of climate factors on GEP*

Figure 6 shows the responses of GEP to climate factors, including soil water content (top layer, 0–5 cm), VPD, air temperature, and global radiation in winter. The GEP increased significantly along with the augmentation of global radiation (Fig. 6d, correlation coefficient: $r = 0.79$, $p < 0.01$), suggesting that solar radiation was an important controlling factor of photosynthesis in winter. As VPD increased with increasing air temperature according to a certain relationship, the response of GEP to VPD (Fig. 6b) was similar to that of air temperature (Fig. 6c). In addition, although a negative correlation existed between surface soil water content and GEP (Fig. 6a), their relationship was not clear because low temperature and weak radiation led to low ground evaporation, to maintain enough soil water for weaker photosynthesis in winter. It indicated that the GEP was weakly influenced by the stomatal behavior. Therefore, photosynthesis was controlled mainly by solar radiation and temperature in winter over the target ecosystem, consistent with observations from Qianyanzhou station (Song et al., 2006).

Compared to that in winter, GEP increased rapidly along with the increase in soil water content ($r = 0.70$, $p < 0.01$) in summer (Fig. 7a), especially under severe drought conditions with soil moisture less than 0.16 m^3 m^{-3} ($r = 0.85$, dashed line in Fig. 7a). This is mainly due to severe soil water deficit limiting the capability for photosynthesis, and

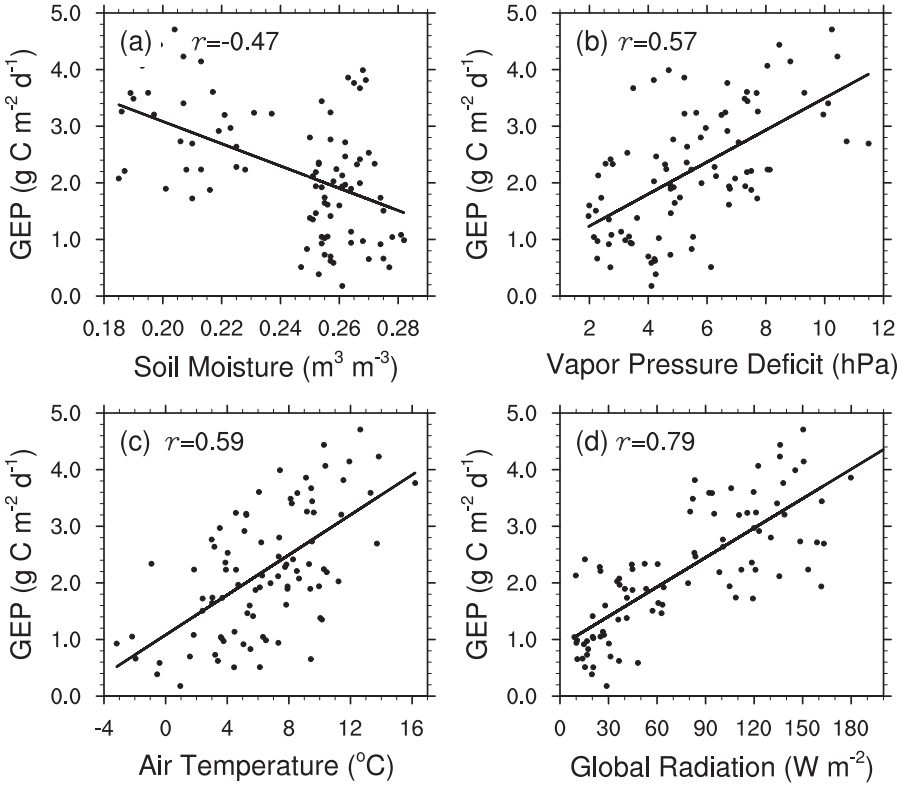

Fig. 6. Responses of GEP to (a) soil moisture, (b) vapor pressure deficit, (c) air temperature, and (d) global radiation in winter. The solid lines represent a linear regression fit, and all the correlation coefficients r are statistically significant ($p < 0.01$).

then affecting the vegetation growth under the conditions of high temperature and intensive radiation in summer (Fig. 3). Meanwhile, GEP decreased along with the increase in VPD (Fig. 7b) and air temperature (Fig. 7c). These negative correlations were even more obvious under the conditions of drought and high temperature stress (dashed lines in Figs. 7b and c), which strengthened the decrease in atmospheric moisture and caused stomatal closure. However, compared to that in winter (Fig. 6d), GEP was not sensitive to incoming global radiation in summer (Fig. 7d), especially for $R_g > 200$ W m^{-2}, because the solar radiation was sufficient during this period, so photosynthesis was limited by the decrease in precipitation (Fig. 3). In summary, GEP was affected mainly by soil moisture, VPD and temperature during the summer drought period and had a weak response to solar radiation.

4.2. *Effect of dry and warm atmospheric conditions on NEE*

To investigate the effect of dry and warm atmospheric conditions on net CO_2 exchange, the relationships between daytime NEE and incoming global radiation sorted into 4°C temperature classes are presented in Fig. 8. Note that 30 minute quality-controlled NEE data were used here to avoid the effect of the gap-filling algorithm, unlike the data used in Figs. 6 and 7 (daily mean data after gap-filling). The regression fit (solid line in Fig. 8) was calculated using a modified Michaelis–Menten equation (Carrara et al., 2004),

$$\mathrm{NEE} = \frac{-a' R_g}{1 - R_g/1000 + a' R_g/\mathrm{GEP_{opt}}} + \mathrm{RE_{day}}\ , \qquad (4)$$

where $\mathrm{GEP_{opt}}$ (μmol m^{-2} s^{-1}) is the optimum GEP at an R_g value of 1000 W m^{-2}; $\mathrm{RE_{day}}$ (μmol m^{-2} s^{-1}) is the daytime ecosystem respiration rate; and a' (μmol J^{-1}) is the ecosystem quantum yield. The values of the three fitted parameters ($\mathrm{GEP_{opt}}$, $\mathrm{RE_{day}}$, a') for the nonlinear regression [Eq. (4)] in Fig. 8 are shown in Table 1. It was easily observed from Fig. 8 that air temperature had a strong effect on the response of daytime NEE to global radiation. From Table 1, we found that the optimum temperature for photosynthesis (maximum $\mathrm{GEP_{opt}}$) was between 20°C and 28°C. The CO_2 uptake rate under optimum radiation ($\mathrm{GEP_{opt}}$) decreased quickly for air temperatures above 24°C (Table 1). $\mathrm{NEE_{opt}}$, the optimum net CO_2 exchange when R_g is 1000 W m^{-2} (defined as $\mathrm{NEE_{opt}} = \mathrm{RE_{day}} - \mathrm{GEP_{opt}}$), is a more precise indicator than $\mathrm{GEP_{opt}}$ because $\mathrm{GEP_{opt}}$ estimates are not robust due to the lack of precision in $\mathrm{RE_{day}}$ values for higher or lower air-temperature classes (Carrara et al., 2004). When the air temperature is higher than 24°C, $\mathrm{NEE_{opt}}$ (absolute value) decreases, consistent with the results from a subtropical coniferous ecosystem in Qianyanzhou (Liu et al., 2006). The observed decrease in $\mathrm{NEE_{opt}}$ may be due to a reduction in GEP or to an increase in RE. High temperatures are typically ac-

Table 1. Parameters of the relationship between the daytime 30 minute quality-controlled net CO_2 ecosystem exchange and incoming global radiation using the Michaelis–Menten model [Eq. (4)], for the data collected in 2013 sorted by 4°C air-temperature class.

Air-temperature class	Num.[a]	GEP_{opt} (μmol m^{-2} s^{-1})	a' (μmol J^{-1})	RE_{day} (μmol m^{-2} s^{-1})	NEE_{opt}[b] (μmol m^{-2} s^{-1})	r_d[c]
$36°C < T_{air} < 40°C$	236	12.96	0.02194	4.52	−8.44	0.65
$32°C < T_{air} < 36°C$	865	19.42	0.05031	5.95	−13.43	0.61
$28°C < T_{air} < 32°C$	1108	22.90	0.05532	4.12	−18.69	0.60
$24°C < T_{air} < 28°C$	857	25.47	0.08901	5.48	−19.83	0.64
$20°C < T_{air} < 24°C$	880	25.69	0.08695	5.02	−20.37	0.57
$16°C < T_{air} < 20°C$	781	20.64	0.09288	4.21	−16.19	0.54
$12°C < T_{air} < 16°C$	663	17.92	0.08642	3.27	−14.71	0.56
$8°C < T_{air} < 12°C$	415	15.23	0.06276	1.68	−12.9	0.49

[a]Num. represents the number of usable 30 minute samples;
[b]NEE_{opt} is the net CO_2 ecosystem exchange at optimum light (incoming global radiation value of 1000 W m^{-2}) defined as $NEE_{opt} = RE_{day} - GEP_{opt}$, where GEP_{opt} is the optimum gross ecosystem production and RE_{day} is the daytime total ecosystem respiration rate;
[c]r_d is the coefficient of determination.

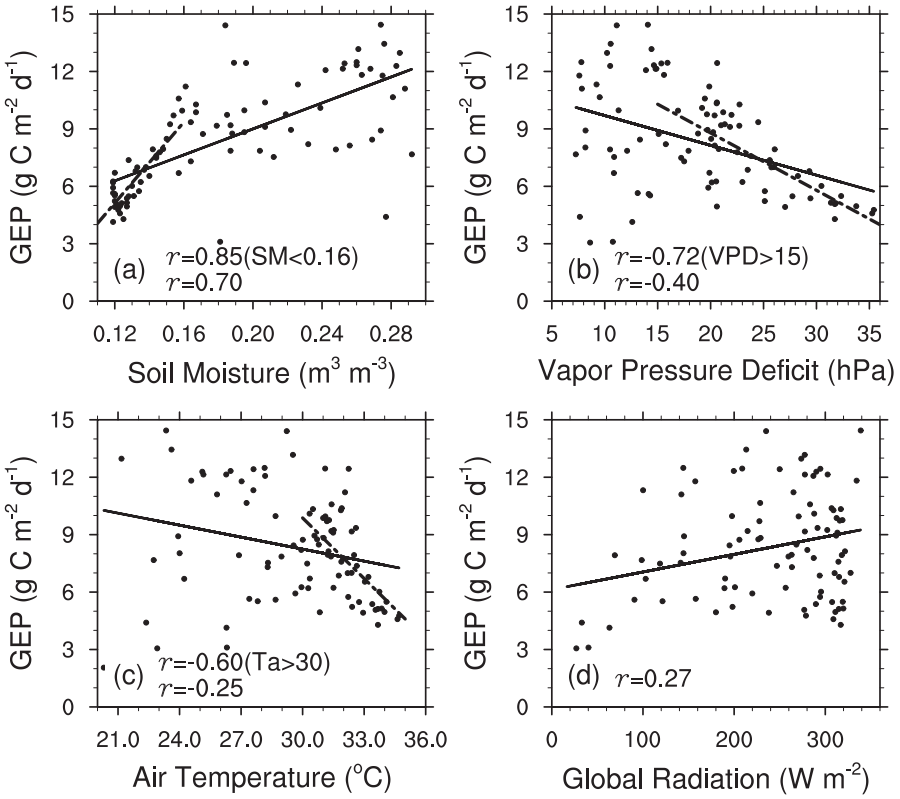

Fig. 7. Responses of GEP to (a) soil moisture, (b) vapor pressure deficit (VPD), (c) air temperature, and (d) global radiation in summer. The dashed lines in (a), (b), and (c) represents conditions of soil moisture < 0.16 m^3 m^{-3}, VPD > 15 hPa, and air temperature $> 30°C$, respectively. All the correlation coefficients R are statistically significant ($p < 0.01$) except the correlation ($r = -0.25$) over the whole air temperature range in (c), with a lower significance level ($p < 0.05$).

companied by high VPD, which could strongly limit photosynthesis through stomatal closure (Farquhar and Sharkey, 1982). Therefore, it was hard to separate the influences of high-temperature stress and drought stress on the decrease in NEE. Here an effort was made to use residual analysis to determine the impacts of temperature and water vapor pressure on NEE (Carrara et al., 2004; Liu et al., 2006).

Figure 9a shows the response of daytime NEE to global radiation as well as the corresponding Michaelis–Menten regression. Clearly, daytime NEE was negatively correlated with global radiation, which can be described by a revised form of the Michaelis–Menten model [Eq. (4)]. In addition, the relationships of air temperature and VPD to the NEE residuals, which are the differences between observed NEE

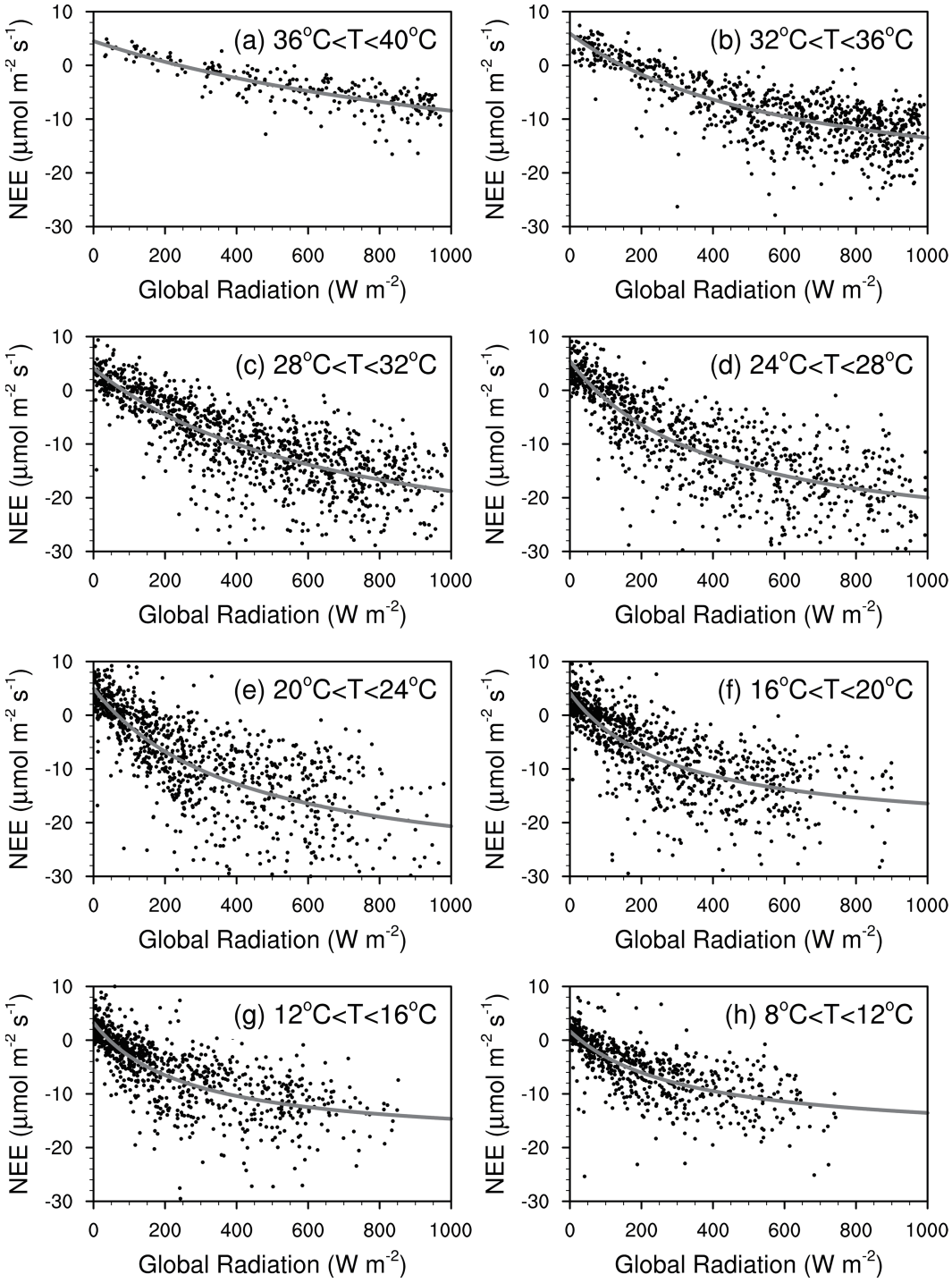

Fig. 8. Relationships between daytime NEE and global radiation in 2013 sorted by 4°C temperature classes. The curves are nonlinear regressions (fitted by a least-squares method) using the modified Michaelis–Menten model [Eq. (4)].

data and the regression values, are presented in Figs. 9b and c. It can be observed that the NEE residuals of the regression strongly depend on air temperature above 30°C as well as on VPD above 15 hPa, consistent with the results shown in Fig. 7. Moreover, above these thresholds, the residuals were more significantly correlated with VPD ($r = 0.51$, $p < 0.001$) than with air temperature ($r = 0.44$, $p < 0.001$). This suggests that VPD was more responsible for the decrease in CO_2 uptake than air temperature under dry and warm atmospheric conditions, as VPD combines the effects of air temperature and relative humidity. It should be noted that the extreme summer drought in 2013 provided an excellent opportunity to study the effect of drought stress on the terrestrial carbon cycle; however, how summer drought affected NEE and its

components is not discussed in depth in this study, but will be addressed in the future.

5. Summary

A new flux tower was established in Ningxiang (eastern Hunan Province) in August 2012, at which CO_2 flux was measured using eddy covariance methods over a subtropical East Asian monsoon mixed forest, representative of a significant portion of the landscape in southern China. Diurnal and seasonal variations of CO_2 fluxes from this site were analyzed for the first time in this study, and their interactions with climate factors were also investigated.

The results showed that the target ecosystem appeared to function as a clear carbon sink in 2013, with integrated NEE, RE, and GEP of −428.8, 1534.8, and 1963.6 g C m^{-2} yr^{-1} respectively. The net carbon uptake (−NEE), RE, and GEP showed obvious seasonal variability, being lower in winter and under drought conditions and higher in the growing season. Carbon uptake was attributed mainly to May, June, and July during the growing season. The maximum net CO_2 uptake occurred on 12 June (7.4 g C m^{-2} d^{-1}), due mainly to appropriate climate conditions for photosynthesis: strong radiation, moderate air temperature, and adequate moisture. An extreme summer drought occurred in July and August, with very low precipitation and high temperature, and this limited photosynthesis through stomatal closure due to higher VPD. This led to a very low net CO_2 uptake in August (9 g C m^{-2} $month^{-1}$), even less than in January (15 g C m^{-2} $month^{-1}$). In addition, obvious diurnal variability was observed for the subtropical mixed forest, and this also changed with the seasons, having a lower amplitude in winter and a higher amplitude during the growing season.

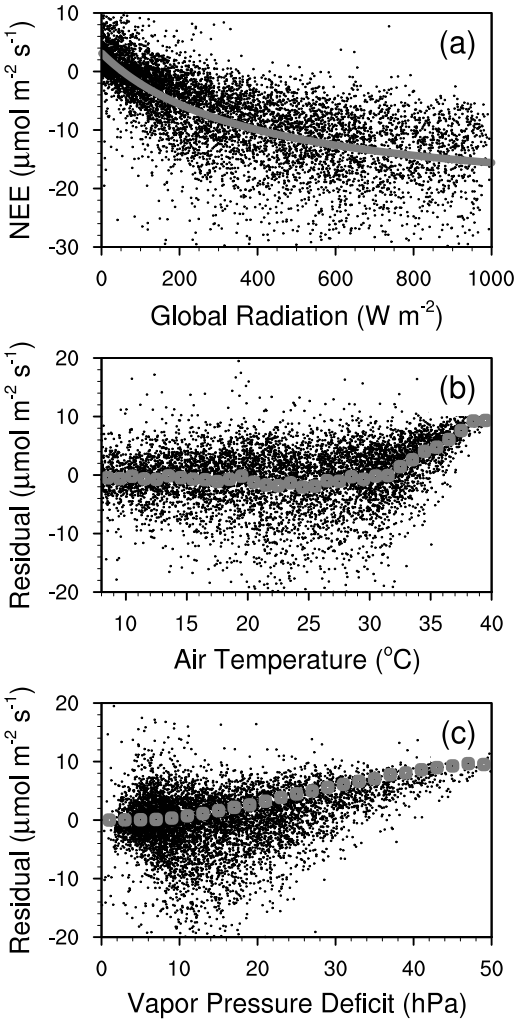

Fig. 9. (a) Relationship between the daytime NEE and global radiation in 2013 (the solid line represents a nonlinear regression using the modified Michaelis–Menten model [Eq. (4)]; (b) residuals of observed NEE data and the regression curve in panel (a) versus air temperature (squares indicate the mean for each 1°C class); and (c) NEE residuals versus vapor pressure deficit (squares indicate the mean for each 2 hPa).

By analyzing the relationships between CO_2 fluxes and climate factors, it was found that solar radiation and temperature were the main controlling factors for GEP in winter, while GEP was affected mainly by soil moisture, VPD, and temperature in summer. In addition, daytime NEE was much more limited by water-stress effect under dry and warm atmospheric conditions than by direct temperature-stress effect. These findings confirmed that the temporal variation of terrestrial carbon exchange fluxes in the East Asian subtropical forest was controlled mainly by climatic factors, consistent with the results of many previous studies (Liu et al., 2006; Song et al., 2006).

Note that the extreme summer drought in 2013 provided an excellent opportunity to study the effect of drought stress on the terrestrial carbon cycle (Zeng et al., 2005; Liu et al., 2006; Zhao and Running, 2010). However, this effect has not been discussed in depth in this study, and it remains a future research topic. Furthermore, our future research will aim to evaluate and improve ecosystem models of biogeochemical and biophysical processes using meteorological and flux data collected at the Ningxiang site.

Acknowledgements. This work was supported by the National Natural Science Foundation of China (Grant Nos. 41305066 and 91125016) and the Special Funds for Public Welfare of China (Grant No. GYHY201306045). The authors gratefully acknowledge the Biogeochemical Integration Department at the Max Planck Institute for Biogeochemistry for making the REddyProcWeb tool available online (http://www.bgc-jena.mpg.de/bgi/index.php/Services/REddyProcWeb). We would like to thank the two anonymous reviewers for their insightful comments that helped to improve the manuscript.

REFERENCES

Aubinet, M., and Coauthors, 2000: Estimates of the annual net carbon and water exchange of forests: The EUROFLUX methodology. *Adv. Ecol. Res.*, **30**, 113–175.

Baldocchi, D., and Coauthors, 2001: Fluxnet: A new tool to study the temporal and spatial variability of ecosystem-scale carbon

dioxide, water vapor, and energy flux densities. *Bull. Amer. Meteor. Soc.*, **82**(11), 2415–2434.

Carrara, A., I. A. Janssens, J. C. Yuste, and R. Ceulemans, 2004: Seasonal changes in photosynthesis, respiration and NEE of a mixed temperate forest. *Agricultural and Forest Meteorology*, **126**, 15–31.

Chen, Z., and Coauthors, 2013: Temperature and precipitation control of the spatial variation of terrestrial ecosystem carbon exchange in the Asian region. *Agricultural and Forest Meteorology*, **182**, 266–276.

Du, Q., H. Liu, J. Feng, and L. Wang, 2014: Effects of different gap filling methods and land surface energy balance closure on annual net ecosystem exchange in a semiarid area of China. *Sci. China (D)*, **57**, 1340–1351.

Falge, E., and Coauthors, 2001: Gap filling strategies for defensible annual sums of net ecosystem exchange. *Agricultural and Forest Meteorology*, **107**(1), 43–69.

Farquhar, G. D., and T. D. Sharkey, 1982: Stomatal conductance and photosynthesis. *Annu. Rev. Plant Physiol.*, **33**, 317–345.

Gao, Z., D. H. Lenschow, Z. He, and M., Zhou, 2009: Seasonal and diurnal variations in moisture, heat and CO_2 fluxes over a typical steppe prairie in Inner Mongolia, China. *Hydrol. Earth Syst. Sci.*, **13**, 987–998.

Joo, S. J., S. U. Park, M. S. Park, and C. S. Lee, 2012: Estimation of soil respiration using automated chamber systems in an oak forest at the Nam-San site in seoul. *Korea. Sci. Total. Environ.*, **416**, 400–409.

Ju, W. M., J. M. Chen, D. Harvey, and S. Wang, 2007: Future carbon balance of China's forests under climate change and increasing CO_2. *Journal of Environmental Management*, **85**, 538–562.

Le Quéré, C., and Coauthors, 2013: The global carbon budget 1959–2011. *Earth System Science Data Discussions*, **5**, 165–185.

Liu, J. G., and Coauthors, 2013: The long-term field experiment observatory and preliminary analysis of land–atmosphere interaction over hilly zone in the subtropical monsoon region of southern China. *Atmos. Oceanic. Sci. Lett.*, **6**, 203–209.

Liu, Y., and Coauthors, 2006: Seasonal dynamics of CO_2 fluxes from subtropical plantation coniferous ecosystem. *Sci. China* (D), **49**(Supp. II), 99–109.

Luo, Y., R. Sherry, X. Zhou, and S. Wan, 2009: Terrestrial carbon-cycle feedback to climate warming: Experimental evidence on plant regulation and impacts of biofuel feedstock harvest. *GCB Bioenergy*, **1**, 62–74.

Lloyd, J., and J. A. Taylor, 1994: On the temperature dependence of soil respiration. *Funct. Ecol.*, **8**, 315–323.

Moffat, A., and Coauthors, 2007: Comprehensive comparison of gap-filling techniques for eddy covariance net carbon fluxes. *Agricultural and Forest Meteorology*, **147**, 209–232.

Papale, D., and Coauthors, 2006: Towards a standardized processing of net ecosystem exchange measured with eddy covariance technique: Algorithms and uncertainty estimation. *Biogeosciences*, **3**, 571–583.

Piao, S., J. Fang, P. Ciais, P. Peylin, Y. Huang, S. Sitch, and T. Wang, 2009: The carbon balance of terrestrial ecosystems in China. *Nature*, **458**, 1009–1013.

Reichstein, M., and Coauthors, 2005: On the separation of net ecosystem exchange into assimilation and ecosystem respiration: Review and improved algorithm. *Global. Change. Biol.*, **11**(9), 1424–1439.

Song, X., G. Yu, Y. F. Liu, X. M. Sun, Y. M. Lin, and X. F. Wen, 2006: Seasonal variations and environmental control of water use efficiency in subtropical plantation. *Sci. China* (D), **49**(Supp. II), 119–126.

Webb, E. K., G. I. Pearman, and R. Leuning, 1980: Correction of flux measurement for density effects due to heat and water vapor transfer. *Quart. J. Roy. Meteor. Soc.*, **106**, 85–100.

Wilczak, J. M., S. Oncley, and S. Stage, 2001: Sonic anemometer tilt correction algorithms. *Bound. -Layer Meteor.*, **99**, 127–150.

Xu, Y., Y. Huang, and Y. Li, 2012: Summary of recent climate change studies on the carbon and nitrogen cycles in the terrestrial ecosystem and ocean in China. *Adv. Atmos. Sci.*, **29**(5), 1027—1047, doi: 10.1007/s00376-012-1206-9.

Yu, G., Y. L. Fu, X. M. Sun, X. F. Wen, and L. M. Zhang, 2006: Recent progress and future directions of ChinaFLUX. *Sci. China* (D), **49**(Supp. II), 1–23.

Yuan, W., Y. Q. Luo, A. Richardson, R. Oren, and S. Luyssaert, 2009: Latitudinal patterns of magnitude and interannual variability in net ecosystem exchange regulated by biological and environmental variables. *Global. Change. Biol.*, **15**, 2905–2920.

Zeng, N., H. F. Qian, C. Roedenbeck, and M. Heimann, 2005: Impact of 1998–2002 midlatitude drought and warming on terrestrial ecosystem and the global carbon cycle. *Geophys. Res. Lett.*, **32**, L22709, doi: 10. 1029/2005GL024607.

Zhao, L., Y. Li, S. Xu, H. Zhou, S. Gu, G. Yu, and X. Zhao, 2006: Diurnal, seasonal and annual variation in net ecosystem CO_2 exchange of an alpine shrubland on Qinghai-Tibetan plateau. *Global. Change. Biol.*, **12**, 1940–1953.

Zhao, M. S., and S. W. Running, 2010: Drought-induced reduction in global terrestrial net primary production from 2000 through 2009. *Science*, **329**, 940–943, doi: 10.1126/science.1192666.

Zheng, X. H., and Coauthors, 2008: Quantifying net ecosystem carbon dioxide exchange of a short-plant cropland with intermittent chamber measurements. *Global Biogeochemical Cycles*, **22**, GB3031, doi: 10.1029/2007GB003104.

Zhu, Z. L., X. M. Sun, X. F. Wen, Y. L. Zhou, J. Tian, and G. F. Yuan, 2006: Study on the processing method of nighttime CO_2 eddy covariance flux data in ChinaFLUX. *Sci. China* (D), **49**(Supp. II), 36–46.